

Irradiation and penetration tests of boron-doped low activation concrete using 2.45 and 14 MeV neutron sources

Atsuhiko Morioka ^{*}, Satoshi Sato, Masaharu Kinno ¹, Akira Sakasai, Junichi Hori, Kentaro Ochiai, Michinori Yamauchi, Takeo Nishitani, Atsushi Kaminaga, Kei Masaki, Shinji Sakurai, Takao Hayashi, Makoto Matsukawa, Hiroshi Tamai, Shinichi Ishida

Japan Atomic Energy Research Institute, 1 Fujita Corporation, Naka Fusion Research Establishment, 801-1, Mukoyama, Naka-machi, Naka-gun, Ibaraki-ken 311-0193, Japan

Abstract

The neutron penetration and the activation characteristics of the boron-doped low activation concrete were investigated for irradiation of 2.45 and 14 MeV neutrons. The shielding property of the 2 wt% boron-doped low activation concrete is superior to that of the 1 wt% boron for the thermal neutron, on the contrary to no clear difference for the fast neutron. The total activity detected in the boron-doped low activation concrete was about one hundredth of that in the geostandard sample at more than 30 days cooling time. The total activity of the boron-doped concrete by major nuclei does not depend on the boron density for the 14 MeV neutron irradiation.

© 2004 Published by Elsevier B.V.

1. Introduction

Activation of structural materials such as concrete in nuclear facilities has been attracted by the special interest, which produce less induced activation. The reductions of those are the important issue in terms of maintenance and decommissioning after shut down of the operation.

The low activation concrete, Wide-use type 1 for the fission reactor [1] is made of white Portland cement and special limestone. The concentrations of silicon, aluminum, iron, magnesium, sodium, potassium, manganese, titanium, and phosphorus of the low activation concrete

are very few compared with the ordinary concrete [1] and with the geostandard sample, JA2 [2].

The boron carbide (B_4C) were doped to the low activation concrete in order to shield the thermal neutrons and reduce the induced activities caused by the thermal neutrons. The boron-doped low activation concrete is to be applied as a neutron shielding material of the cryostat for DD fusion device [3,4]. The activities of ^{41}Ar produced by $^{40}Ar(n,\gamma)$ reaction in the JT-60 torus hall were estimated by the DD operation. It was found that the activity of ^{41}Ar nuclide with the boron-doped concrete was reduced by about 90% in comparison with the ordinary concrete [5]. This paper will be reported into the following points.

- Irradiation tests of boron-doped low activation concrete by 2.45 and 14 MeV neutrons were performed to investigate the neutron penetration and the activation characteristics using FNS (fusion neutronics source) facility in Japan Atomic Energy Research Institute [6]. In the penetration experiments, the

^{*} Corresponding author. Tel.: +81-29 270 7448/7328/7419; fax: +81-29 270 7419.

E-mail address: morioka@naka.jaeri.go.jp (A. Morioka).

¹ Address: 1: 4-25-2, Sendagaya, Shibuya-ku, Tokyo, 151-8570 Japan.

calculation results were compared with the experiment ones using Monte Carlo calculation code, MCNP-4C2 [7], with the continuous energy cross section data sets based on the JENDL-3.2 [8].

- The induced activity of the boron-doped low activation concrete and the geostandard sample were evaluated for DT neutron irradiation.

2. Boron-doped low activation concrete

The boron carbide was doped to the low activation concrete. The boron-doped low activation concrete including the natural boron with 1 and 2 wt% concentrations, which are named as B1 and B2, respectively, were prepared. The chemical compositions of the boron-doped low activation concrete (B1 and B2) and the geostandard sample, JA2, are summarized in Table 1.

Table 1
Chemical composition of B1, B2 and JA2 (wt%)

	1 wt% Boron (B1)	2 wt% Boron (B2)	Geostandard (JA2)
H	1.5	1.5	0.26
Si	2.9	2.9	26
Ca	36	36	4.5
Al	0.65	0.65	8.2
Fe	0.063	0.062	4.4
Mg	0.26	0.26	4.6
Na	0.04	0.04	2.3
K	0.029	0.029	1.5
Mn	6.3×10^{-4}	6.4×10^{-4}	0.084
Ti	5.0×10^{-3}	4.9×10^{-3}	0.4
P	3.7×10^{-4}	3.6×10^{-6}	0.064
C	7.3	7.4	–
S	0.28	0.28	–
B	1.0	2.1	–
O	50	49	47

3. Neutron penetration tests

3.1. Assembly for neutron irradiation

Two pieces of test concrete for each B1 and B2, 40 cm × 40 cm × 10 cm in size, weighing 36.5 kg, were prepared. The experimental assembly used for the irradiation test of DD neutrons is illustrated in Fig. 1. The collimated neutrons are irradiated to the assembly in the first target room at FNS. The neutron flux through the boron-doped low activation concrete was measured by ^{238}U fission chamber for fast neutrons above 1 MeV and by ^3He proportional counter for thermal neutrons. These chambers were placed at 0.0, 10.0 and 20.0 cm distance from the test concrete along the central axis of the assembly.

3.2. Results and discussion

The count rates measured by ^{238}U fission chamber in B1 and B2 concrete are shown in Fig. 2 together with the MCNP calculation of B1 concrete. The circle and triangle keys indicate the measured results for the B1 and B2, respectively. Calculated results for B1 by MCNP are also shown by the solid line.

The experimental results show that the fast neutron shielding property of B2 is almost same as B1 within experimental error. The calculation results were compared with the experiment ones using the Monte Carlo calculation code, MCNP-4C2. The calculation results agree well with the experimental results within 10%. Calculated results for B2 by MCNP were nearly the same as those for B1. The experimental result show that the fast neutron fluxes through the boron-doped low activation concrete does not depend on the boron density.

The penetration experiments of the thermal neutron were performed by placing the polyethylene plate of 20 cm thickness in front of the test concrete.

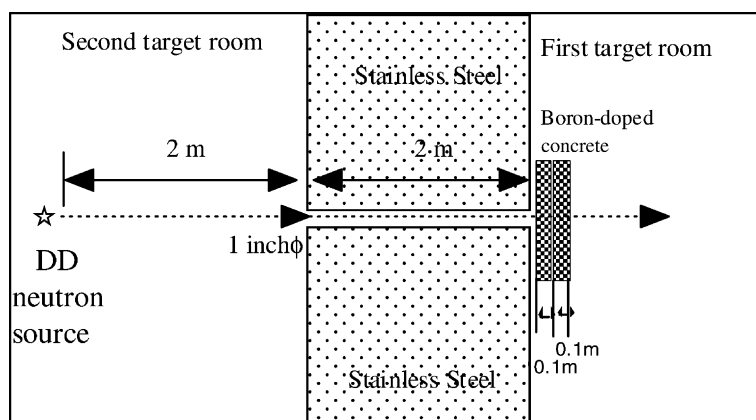


Fig. 1. Experimental assembly used for the DD neutron penetration experiment.

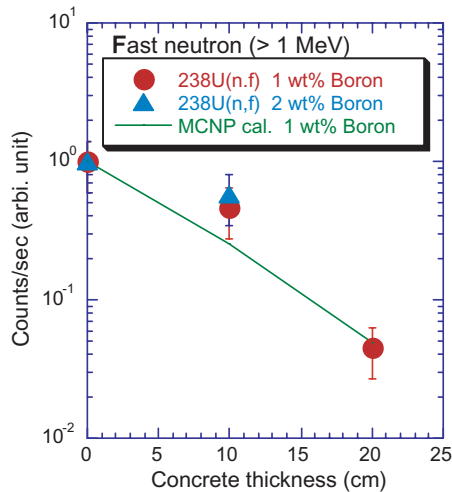


Fig. 2. Count rates measured by ^{238}U fission chamber in B1 and B2 concretes, and MCNP calculation in B1.

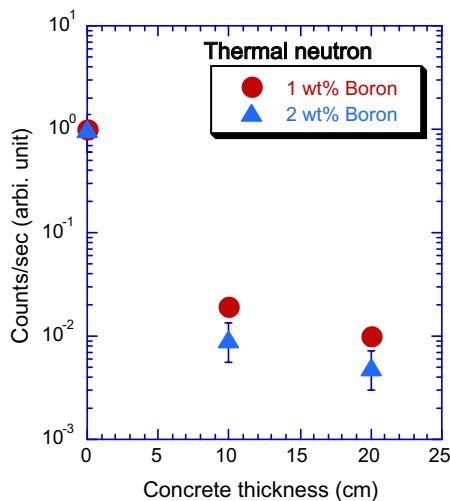


Fig. 3. Count rates measured by ^3He proportional counter in B1 and B2 concretes.

Fig. 3 shows the count rates by the ^3He proportional counter for B1 (circles) and B2 (triangles). It was experimentally clarified that the thermal neutron flux of B2 was about a half of B1. This means that the shielding property of thermal neutron for B2 is superior to that for B1.

4. Induced activities of the boron-doped low activation concrete

4.1. Experiment method

The DD neutron irradiation tests were mainly performed using the 0° beam line of the FNS at the same

time of the penetration tests. The B1 specimens, weighing 0.17 g, were directly attached to the Ti–D target assembly.

In DT neutron irradiation test, the powdered B1, B2 and JA2 specimens with $50\text{ mm} \times 50\text{ mm} \times 1\text{ mm}$ were prepared. The $^{93}\text{Nb}(n, 2n)^{92\text{m}}\text{Nb}$ reaction is suitable to examine the integral neutron flux above 10 MeV. As a neutron fluence monitor by DT neutron irradiation tests, the niobium foils with $50\text{ mm} \times 50\text{ mm} \times 0.1\text{ mm}$ were attached to the specimens.

The DT neutron irradiation tests were mainly performed using the 80° beam line of the FNS. The DT neutron yield was monitored by a silicon surface barrier diode (SSD) using the associated alpha particle measurements. DT neutron at the target was about 1.3×10^{11} neutrons/s on average. Since the specimens were directly attached to the Ti–T target assembly.

Two continuous irradiation tests for 6 h were performed. The induced activities of the specimens were measured by gamma-ray spectroscopy with the high purity Ge detector at the time of specimen cooling from 7 days to 6 months.

4.2. Results and discussion

From gamma ray spectrum of the irradiated specimens, the dominant radionuclides induced in various materials in boron-doped low activation concrete and the geostandard sample are identified. The typical gamma ray spectrums for the B1 specimen at the time of 2 and 20 h cooling after the DD neutron irradiation are indicated in Fig. 4. The nuclides of ^{24}Na were detected in the B1 specimens. Although the gamma ray of 389 keV of $^{87\text{m}}\text{Sr}$ could be observed at the time of 2 h cooling, it could not be observed at the time of 20 h cooling.

Fig. 5 shows the measured gamma ray spectra for the B1 specimen at the time of cooling of 7 and 97 days after the DT neutron irradiation. The high-energy neutrons resulting from 14 MeV source greatly increases the importance of reactions such as (n, p), (n, 2n) reactions having thresholds upper them 10 MeV range. In the measured gamma ray spectra, the induced activities were evaluated by each radioactive nuclide in B1, B2 and JA2 as a function of the cooling time. The dominant nuclides in the B1, B2 and JA2 were ^{22}Na , ^{24}Na , ^{47}Ca , ^{46}Sc , ^{47}Sc , ^{48}Sc , ^{51}Cr , ^{54}Mn and ^{58}Co . The measured induced activities of the B1 specimen as a function of the cooling time after the DT neutron irradiation are shown in Fig. 6.

The nuclides of ^{24}Na are produced by $^{23}\text{Na}(n, \gamma)$, $^{24}\text{Mg}(n, p)$ and $^{27}\text{Al}(n, \alpha)$ reactions. The nuclides of ^{47}Ca are produced by $^{46}\text{Ca}(n, \gamma)^{47}\text{Ca}$ and $^{48}\text{Ca}(n, 2n)^{47}\text{Ca}$. The nuclide of ^{47}Sc is mainly produced by β -decay of ^{47}Ca .

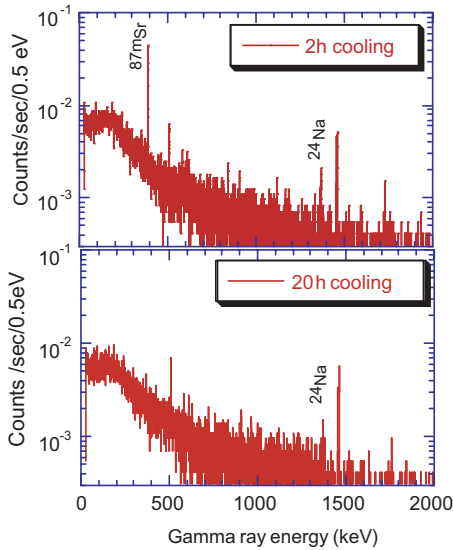


Fig. 4. Gamma ray spectrum for B1 specimen at the time of cooling of 2 and 20 h after the DD neutron irradiation.

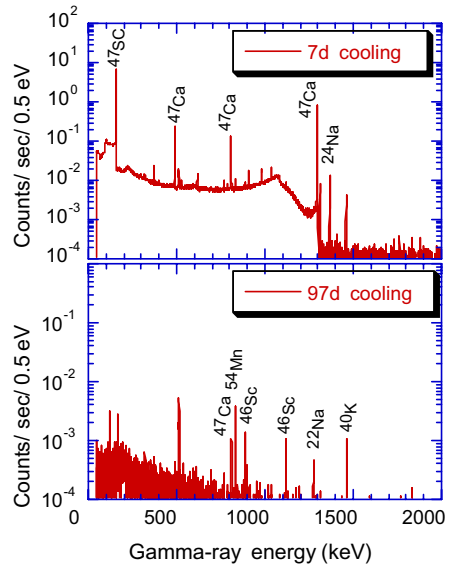


Fig. 5. Gamma ray spectrum for B1 specimen at the time of cooling of 7 and 97 days after the DT neutron irradiation.

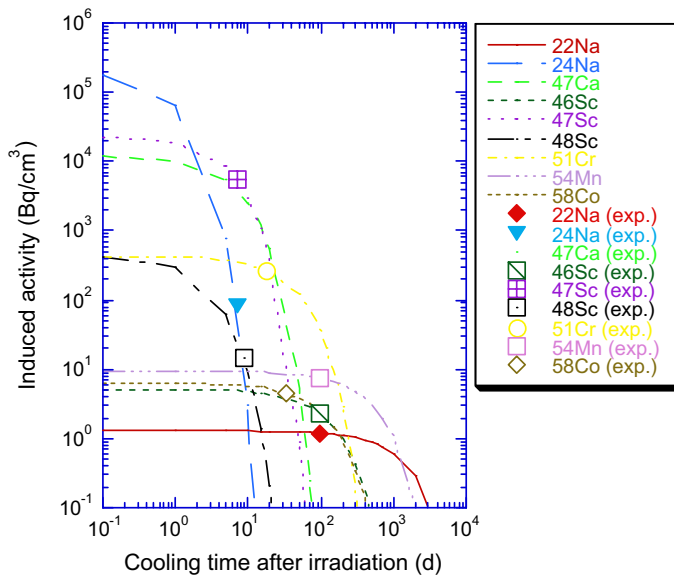


Fig. 6. Induced activity for B1 specimen as a function of cooling time after DT neutron irradiation.

The sum of the induced activities of the dominant nuclides detected in the specimens of B1, B2 and JA2 are indicated in Fig. 7 after the DT neutron irradiation.

The total activity by major nuclei of the boron-doped low activation concrete does not depend on the boron density. The total activities detected in B1 and B2 are lower than that in JA2 during one-day cooling period and later than 4 weeks cooling. The concentrations of

sodium and manganese in B1 and B2 are very few compared with those of JA2 so that ^{22}Na , ^{24}Na and ^{54}Mn in B1 and B2 are lower than those of JA2. During 7–10 day cooling time, those in B1 and B2 are higher than JA2. The concentration of calcium of B1 and B2 are larger than that of JA2 so that ^{47}Ca , ^{47}Sc and ^{48}Sc in B1 and B2 are large compared with those of JA2 [9].

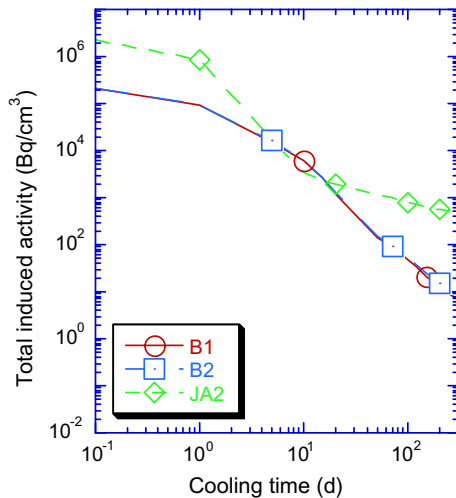


Fig. 7. The sum of induced activities detected in the specimens of B1, B2 and JA2.

The results show that the reduction of the radionuclides of ^{47}Ca and ^{48}Sc , in a case of short period of operation, is important to reduce the dose rate at the cooling time of 1 week.

5. Conclusion

The DD and DT neutron irradiation tests were performed for the evaluation of these penetrations and the induced activity of the boron-doped concrete.

- The fast neutron penetration through the boron-doped concrete does not depend on the boron density. On the other hands, the shielding property of thermal neutron of 2 wt% boron-doped concrete is superior to that of 1 wt% boron-doped concrete.
- The induced activities of the boron-doped concrete, B1 and B2, and the geostandard sample, JA2, were evaluated.

- The total activity by major nuclei of the boron-doped concrete does not depend on the boron density.
- The total activity detected in the B1 and B2 was about one hundredth of that in the geostandard sample at more than 30 days cooling time, because the nuclides of ^{22}Na , ^{24}Na and ^{54}Mn in the B1 and B2 are lower than those of the JA2. During 7–10 days cooling time, the total activity in the B1 and B2 is higher than that in the geostandard sample, because the nuclides of ^{47}Ca and ^{48}Sc in the boron-doped concrete are larger than the JA2. It can be concluded the boron-doped low activation concrete is very attractive as a shielding material of the cryostat of the DD fusion reactor. However, for the DT fusion reactor, in a case of short period of operation, it will be necessary to reduce the quantity of the calcium.

Acknowledgements

The authors wish to acknowledge C. Kutsukake, S. Tanaka, Y. Abe, M. Seki and Y. Oginuma for operation of the FNS accelerator.

References

- [1] M. Kinno et al., J. Nucl. Sci. Technol. (Suppl. 1) (2000) 821.
- [2] N. Imai et al., Geostandard. Newslett. 19 (1995) 135. Available from <<http://www.aist.go.jp/RIODB/geostand/igneous.html>>.
- [3] M. Matsukawa et al., Fusion Eng. Des. 63&64 (2002) 519.
- [4] S. Ishida et al., Nucl. Fusion 43 (2003) 606.
- [5] A. Morioka et al., Fusion Eng. Des. 63&64 (2002) 115.
- [6] <http://www.fnshp.tokai.jaeri.go.jp>.
- [7] Judith F. Briesmeister, MCNP - A General Monte Carlo N-Particle Transport Code Version 4C, LA-13709-M (2000).
- [8] IAEA-NDS-110. Rev.5, Japan, 1994.
- [9] S. Sato et al., J. Nucl. Sci. Technol. (Suppl. 4) (2004) 66.